Traveling Wave Based Single-Phase-to-Ground Protection Method for Power Distribution System

Xinzhou Dong, *Member, CSEE, Senior Member, IEEE*, Jun Wang, Shenxing Shi, *Member, CSEE, Member, IEEE*, Bin Wang, *Member, CSEE, Member, IEEE*, Bak Dominik, and Miles Redefern

***Abstract*—Correct detection and identification of single-phase to-ground faults not effectively grounded in distribution systems is a major challenge for protection engineers. This paper proposes a novel traveling wave based protection method to solve this problem. The proposed method compares the polarities of current and voltage traveling waves measured immediately after the fault inception to determine the fault direction. Nuisance tripping is avoided by using the power frequency voltages detected on the busbar to inhibit operation. The power frequency voltages ensure that the system does not mal-operate due to noise and also provide discrimination for phase-to-phase and three-phase faults. The wavelet transform and modulus maxima theories are used to extract the polarity of traveling waves measured at the relaying point. The simulation studies demonstrate correct operation of protection, which is independent of fault distance, fault inception angle, fault path resistance, and the method used for neutral grounding.**

***Index Terms*—Distribution systems, relay protection, single-phase-to-ground fault, traveling wave, wavelet transform.**

I. Introduction

POWER distribution systems, which are mostly either isolated from ground or use high impedance grounding, are widely encountered in many countries. In case of an isolated system, when a single-phase-to-ground fault occurs, the fault current, which flows from busbar through protection point to the faulted line, has a very small magnitude, creating significant challenges for detection and providing effective protection against single-phase-to-ground faults.

Several schemes have been proposed to identify single-phase-to-ground faults in non-effectively grounded power distribution systems. Some traditional methods [1]–[4] that focus on power frequency currents include watt-metric method, admittance method, negative sequence current method, and harmonic-based method. However, all of these schemes are not always successful, especially when the magnitude of an actual fault current is relatively small. Field tests have proven that these methods cannot provide the required dependability and sensitivity of operation. Therefore, they are not able to fulfill the requirements of satisfactory operation [5], [6].

Injection methods have been also proposed [7], [8]. However, these methods require extra hardware to be fitted into the power system, which makes for difficulties in implementation.

Fault generated transient signals have been used to detect faults on transmission systems for many years, but their application to detect single-phase-to-ground faults on distribution networks is relatively new. The detection system analyzes the fault information by filtering the fault generated power frequency currents [9], [10].

In order to highlight fault characteristics, faulted feeder selection technology, which compares the characteristics of the faulty feeder against healthy ones to identify the faulty feeder, has been proposed [11]. A traveling wave based faulty feeder selection method has shown to drastically improve the accuracy of selecting the feeder with a single-phase-to-ground fault [12]. However, the faulty feeder selection technique needs to acquire fault-generated information in all feeders connected to the same busbar. In this manner, it can provide network protection rather than concentrating on an individual feeder.

The fault generated traveling wave is a transient signal with clear physical meaning and is not dependent on the method of neutral grounding. The first relays using fault-generated transients to detect faults were introduced in the mid-1930s [13]. However, it was not until the 1970s, that the traveling wave relay RALDA [14] was largely employed. Unfortunately, this relay was prone to nuisance operations, and was triggered by lightning strokes and switching operations. Recently, several algorithms for analyzing traveling waves have been proposed, and new traveling wave and fault generated transient based relays have been developed [15]–[17]. However, all of these have been intended for the protection of transmission systems.

In this paper, a traveling wave based single-phase-to-ground protection method for power distribution systems is proposed. The protection utilizes the wavelet transform and modulus maxima. It extracts the polarity of initial current and voltage traveling waves and identifies the fault by the polarity comparison of modulus maxima. Busbar voltages are used to distinguish single-phase-to-ground from phase-to-phase faults and also to prevent nuisance tripping. The proposed protection can be widely used in different power distribution systems and works correctly in most fault conditions.

This paper is organized as follows. Section II includes basic principles of the traveling wave based single-phase-to-ground protection. Section III contains a discussion on power distribution system. Section IV provides a protection distribu-

Manuscript received March 25, 2015; revised May 31, 2015; accepted June 8, 2015. Date of publication June 30, 2015; date of current version May 20, 2015. This work was financed by the National Natural Science Foundation of China under Grant 50930072, 51120175001, 51477084, and in part by the Beijing Natural Science Foundation under Grant 3152016.

X. Dong, S. Shi, B. Wang, B. Dominik are with the Tsinghua University, Beijing 100084, China (e-mail: xzdong@tsinghua.edu.cn, shishenxing@mail.tsinghua.edu.cn, binw_ee@mail.tsinghua.edu.cn, dominikjanbak@o2.pl).

J. Wang is with the Electric Power Planning & Engineering Institute, Beijing 100120, China (e-mail: junwang@cpecc.net).

M. Redefern is with the University of Bath, Bath, UK (e-mail: m.a.redfern@bath.ac.uk)

Digital Object Identifier 10.17775/CSEEJPES.2015.00022

tion system. Section IV provides a protection algorithm. Section V provides simulation and evaluation using electromagnetic transients analysis program (EMTP). Conclusions and references close this paper.

II. Protection Principle

A. Basic Principle

When a single-phase-to-ground fault occurs in the power distribution system, fault generated traveling waves will propagate from the fault point to busbar along the faulty feeder. At the busbar, where the value of wave impedance changes, the traveling wave gets reflected and refracted.

According to the traveling wave transmission theory, the voltage reflected and refracted traveling waves can be written as

$$\begin{cases} u_{\mathrm{z}} = \dfrac{2z_2}{z_1+z_2}u_{\mathrm{r}} \\ u_{\mathrm{f}} = \dfrac{z_2-z_1}{z_1+z_2}u_{\mathrm{r}} \end{cases} \tag{1}$$

where u_{r}, u_{f} and u_{z} are the voltage incident, reflected and refracted traveling waves, respectively. z_1 and z_2 are the surge impedances of feeders with the incident and refracted traveling waves, respectively.

To simplify calculations, the surge impedances of all the feeders are assumed similar, which yields

$$z_2 = \frac{1}{n-1}z_1 \tag{2}$$

where n is the number of feeders. Then, u_{f} and u_{z} in (1) can be rewritten as

$$\begin{cases} u_{\mathrm{z}} = \dfrac{2}{n}u_{\mathrm{r}} \\ u_{\mathrm{f}} = \dfrac{2-n}{n}u_{\mathrm{r}}. \end{cases} \tag{3}$$

A current traveling wave propagating from busbar to feeder is defined as positive, and propagating from feeder to busbar as negative. As both the current and voltage incident traveling waves propagate from feeder to busbar, then

$$u_{\mathrm{r}} = -z_1 i_{\mathrm{r}}. \tag{4}$$

Since the initial current traveling wave in a faulty feeder results from the superposition of incident and reflected waves while there is only the refracted one in the healthy feeder, then combining (3) and (4) gives

$$\begin{cases} i_{\mathrm{F}} = -\dfrac{2(n-1)}{n}\dfrac{u_{\mathrm{r}}}{z_1} \\ i_{\mathrm{N}} = \dfrac{2}{n}\dfrac{u_{\mathrm{r}}}{z_1} \\ u_{\mathrm{M}} = \dfrac{2}{n}u_{\mathrm{r}} \end{cases} \tag{5}$$

where i_{F} and i_{N} are the initial current traveling waves measured in faulty and healthy feeders, respectively. u_{M} is the initial voltage traveling wave measured at the busbar.

From (5), one can see that the initial voltage and current traveling waves have opposite polarities in a faulty feeder, while they are the same in a healthy feeder. By comparing the polarities of the initial current and voltage traveling waves, the occurrence of a single-phase-to-ground fault can be determined.

B. Principle in Three-Phase Distribution System

It can be proved that the phase-to-modal transformations can still be used to decouple non-transposed electric lines with acceptable accuracy. The demonstration is attached in the appendix. The Karenbauer transformation has been used in this research. The transformation matrices are given as

$$\begin{aligned} \begin{pmatrix} u_0 \\ u_\alpha \\ u_\beta \end{pmatrix} &= \frac{1}{3}\begin{pmatrix} 1 & 1 & 1 \\ 1 & -1 & 0 \\ 1 & 0 & -1 \end{pmatrix}\begin{pmatrix} u_{\mathrm{a}} \\ u_{\mathrm{b}} \\ u_{\mathrm{c}} \end{pmatrix}\begin{pmatrix} i_0 \\ i_\alpha \\ i_\beta \end{pmatrix} \\ &= \frac{1}{3}\begin{pmatrix} 1 & 1 & 1 \\ 1 & -1 & 0 \\ 1 & 0 & -1 \end{pmatrix}\begin{pmatrix} i_{\mathrm{a}} \\ i_{\mathrm{b}} \\ i_{\mathrm{c}} \end{pmatrix} \end{aligned} \tag{6}$$

where u_{a}, u_{b}, u_{c}, i_{a}, i_{b}, and i_{c} are the voltage and current of the phases A, B, and C, respectively. u_α, u_β, i_α, and i_β are the line-modal components of a voltage and current, respectively. u_0 and i_0 are the zero-modal components of a voltage and current, respectively.

If a phase A to ground fault occurs in a feeder, the faulted power system can be divided into a normal operation load system and a fault superimposed system [18]. In the fault superimposed system, the boundary condition of single-phase-to-ground fault can be written as

$$\begin{cases} i_{\mathrm{bf}} = 0 \\ i_{\mathrm{cf}} = 0 \\ u_{\mathrm{af}} = -u_{\mathrm{aF}} \end{cases} \tag{7}$$

where i_{bf} and i_{cf} are the initial current traveling wave of phase B and C, respectively. u_{af} is the initial voltage traveling wave of phase A. u_{aF} is the instantaneous voltage of phase A when the fault has occurred.

Using the Karenbauer transformation to decouple the three phase system, (7) can be rewritten as

$$\begin{cases} i_{0\mathrm{f}} - 2i_{\alpha\mathrm{f}} + i_{\beta\mathrm{f}} = 0 \\ i_{0\mathrm{f}} + i_{\alpha\mathrm{f}} - 2i_{\beta\mathrm{f}} = 0 \\ u_{0\mathrm{f}} + u_{\alpha\mathrm{f}} - u_{\beta\mathrm{f}} = -u_{\alpha\mathrm{F}}. \end{cases} \tag{8}$$

Since the modal components are independent from each other, the following equation is achieved

$$\begin{cases} u_{0\mathrm{f}} = -z_0 i_{0\mathrm{f}} \\ u_{\alpha\mathrm{f}} = -z_\alpha i_{\alpha\mathrm{f}} \\ u_{\beta\mathrm{f}} = -z_\beta i_{\beta\mathrm{f}}. \end{cases} \tag{9}$$

Because the surge impedances of line-modal components are equal to each other, by solving (8) and (9), the incident traveling waves can be written as

$$\begin{cases} u_{0\mathrm{f}} = -\dfrac{z_0}{z_0+2z_\alpha}u_{\mathrm{aF}} \\ u_{\alpha\mathrm{f}} = u_{\beta\mathrm{f}} = -\dfrac{z_\alpha}{z_0+2z_\alpha}u_{\mathrm{aF}} \\ i_{0\mathrm{f}} = i_{\alpha\mathrm{f}} = i_{\beta\mathrm{f}} = \dfrac{1}{z_0+2z_\alpha}u_{\mathrm{aF}}. \end{cases} \tag{10}$$

Considering (5) and (10) for the zero-modal network, u_{r} is equal to $u_{0\mathrm{f}}$, while for line-modal network, u_{r} is equal to $u_{\alpha\mathrm{f}}$ and $u_{\beta\mathrm{f}}$.

The theoretical analyses above prove that both the zero-modal and line-modal components of traveling waves can be used to construct the protection criteria.

C. Selection of Modal Component

When a solid fault with a fault inception angle of 90° occurs in a 35 kV power distribution system, which is the most sensitive situation for traveling wave based protection, the instantaneous voltage in the faulty phase is 28.58 kV. Assume the line-modal surge impedance is 350 and the zero-modal surge impedance is 750 Ω. According to (10), the initial current traveling wave of zero-modal and line-modal components can be derived and their magnitudes will be both 19.7 A.

Assume that the magnitude of a normal load current is about 300 A; then the maximum fault current could be even larger. The initial current traveling wave of the 19.7 A is much smaller than the fault current, and it would be difficult to distinguish it from the noise. However, under normal conditions, there would be no zero-sequence power frequency load or fault current in a non-effectively grounded system. Therefore, the sensitivity of the zero-sequence measurement can be increased ensuring that the zero-modal traveling wave can be resolved.

Based on the analysis above, the zero-modal component is selected to implement the protection.

III. Further Discussion on Distribution System

There are two further complications in the use of traveling wave based protection in distribution systems. The first is the usage of a voltage transformer and its operation in the frequency range associated with traveling waves. The second one is the reliability with which traveling wave based protection can be distinguished from high frequency waves generated by the breaker's operations, lightning strokes, and other forms of electromagnetic interference.

A. Transmission Character of Transformers

The electromagnetic potential transformer (PT) and electromagnetic current transformer (CT) are widely used in power distribution systems. The theoretical analysis and the successful applications of traveling wave based fault location and faulted feeder selection technology in the field both demonstrate that CT can effectively transfer high frequency signals of traveling waves [19]. Moreover, as recent theoretical studies and experiments have verified, a significant electrostatic perceptual phenomenon occurs when high frequency signals pass through PT. In this manner, the voltage traveling wave can be transmitted via this electrostatic perceptual phenomenon without delay [20]–[22].

Based on the above fact, both the initial voltage and current traveling waves signals can be transduced through PT and CT, respectively.

B. Further Improvements for the Reliability of Protection

Traveling waves are high-frequency transient signals, and it is difficult to distinguish them from noise and other high frequency waves that exist in power system, such as lightning strokes and switching transients. This is the main reason why traveling wave based protection is prone to nuisance tripping. In order to improve the reliability and avoid mal-operation, the power frequency zero-sequence voltage detected on the busbar has been used to block the protection.

During a single-phase-to-ground fault, a power frequency zero-sequence voltage can be detected on the busbar. This voltage will remain until the fault has been isolated. When high-frequency noise or other transient generated waves lead to false diagnosis using the traveling wave based protection criteria, the power frequency zero-sequence voltage will be absent. Therefore, the protection uses the traveling wave principle to determine the direction of fault and detecting power frequency zero-sequence voltage to avoid mal-operation.

C. Identification of Single-Phase-to-Ground Fault

The polarity criteria of the initial current and voltage traveling waves is also satisfied for two-phase-to-ground faults. However, in a power distribution system, the traditional power frequency parameter based protection devices has excellent operational characteristics. In order to avoid the impact of a traveling wave based protection on traditional protection, the traveling wave based single-phase-to-ground protection should be blocked for other faults. Of course, the blocking criteria mentioned in Section III. B can block phase-to-phase and three-phase faults. As for two-phase-to-ground fault, a sequence voltage based phase selection method is adopted [23].

IV. Protection Algorithm

A. Wavelet Transform

The discrete dyadic wavelet transform has been widely used in analyzing traveling wave signals. These can be decomposed into wavelet components and approximation components under different scales, which can reflect different frequency bands of signals [24]. Discrete sequence $f(n)$ based on discrete dyadic wavelet transform can be written as

$$\begin{cases} A^d_{2^j} f(n) = \sum_k h_k A^d_{2^{j-1}} f(n - 2^{j-1}k) \\ W^d_{2^j} f(n) = \sum_k g_k A^d_{2^{j-1}} f(n - 2^{j-1}k). \end{cases} \tag{11}$$

$A^d_{2^j} f(n)$ and $W^d_{2^j} f(n)$ are the approximation and wavelet components at the scale 2^j. $\{h_i\}_{i\in Z}$ and $\{g_i\}_{i\in Z}$ are wavelet coefficients determined by wavelet function.

In this paper, the derivative function of the cubic B-spline function is used as a wavelet function, as its numerical realization is the simplest one among all the other spline functions and can be easily approximated with Gauss function. For the aforementioned wavelets, the coefficients are $\{h_k\} = (0.125, 0.375, 0.375, 0.125)$ $(k = -1, 0, 1, 2)$ and $\{g_k\} = (-2, 2)$ $(k = 0, 1)$.

The modulus maxima of wavelet transforms are used to represent the polarities of traveling waves, and its definition is, $\forall \varepsilon > 0$, a neighborhood $|t - t_0| < \varepsilon$ exists; for every $t \neq t_0$,

$$|W(2^j, t_0)| \geq |W(2^j, t)|. \tag{12}$$

B. The Wavelet Representation of Traveling Waves

The wavelet representation of traveling waves was demonstrated using the EMTP and the simplified radial power distribution system shown in Fig. 1.

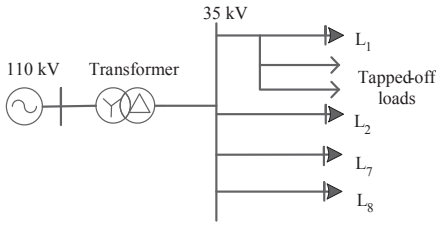

Fig. 1. A simplified 35 kV radial distribution system.

Eight feeders from L_1 to L_8 are connected to the busbar. The three phase lines are not transposed. The neutral is ungrounded. The Jmarti line module is used with the line structure shown in Fig. 2. The electric network data are detailed in the appendix.

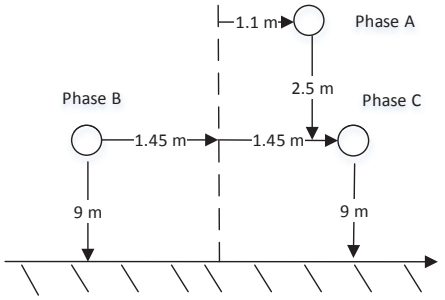

Fig. 2. A typical power distribution line.

A phase A to ground fault was applied to feeder L_2, 5 km from the busbar with a fault arc resistance of 100 Ω.

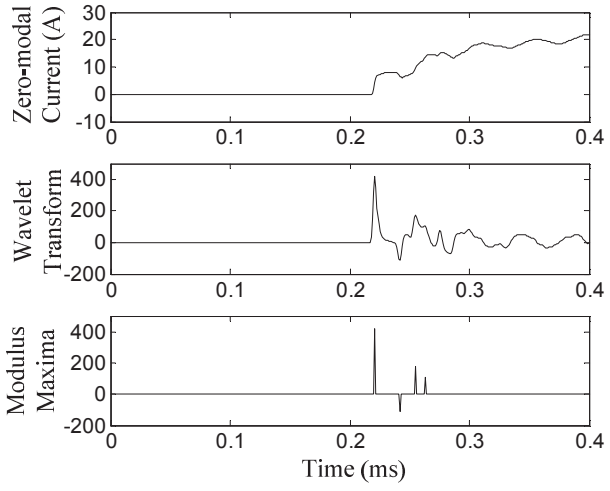

Fig. 3. Current traveling wave, its wavelet transformation and modulus maximum measured in a faulty feeder.

The zero-modal current traveling wave, as well as its wavelet transform and the modulus maxima are illustrated in Fig. 3 in the case of a faulty feeder and in Fig. 4 for a healthy one. Fig. 5 illustrates, in turn, the zero-modal voltage traveling wave as well as its wavelet transform and modulus maxima, respectively. As can be seen from Fig. 3, 4, and 5, the information of the amplitude and polarity of traveling waves is concisely combined into modulus maxima. It can also be seen that the initial polarities of the voltage and current modulus maxima are opposite for faulty and healthy feeders, which can be used to indicate fault conditions.

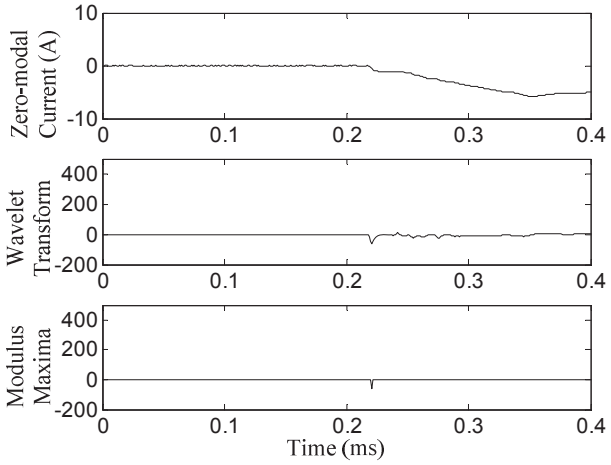

Fig. 4. Current traveling wave, its wavelet transform and maximum modulus measured in a healthy feeder.

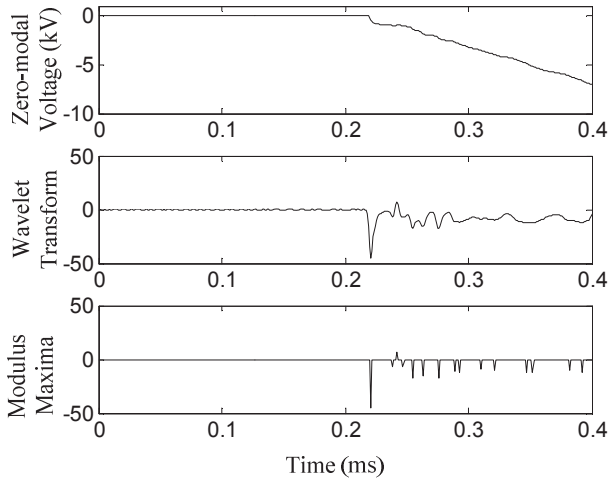

Fig. 5. Voltage fault traveling wave, its wavelet transform and maximum modulus measured at a busbar.

C. Scale Selection

The challenge of using the zero-modal traveling wave is that it is heavily attenuated on long feeders and that this situation can be made even worse by a fault path's resistance.

In order to assess the attenuation of zero-modal traveling waves, the line constant program in EMTP is used to calculate the line unit resistance for different frequencies. The line structure is shown in Fig. 2.

From Table I, it is clear that the line's unit resistance for a zero sequence increases greatly as the signal's frequency increases, which results in higher attenuations of zero-modal traveling waves in the higher frequency bands.

TABLE I
THE ZERO SEQUENCE LINE UNIT RESISTANCE IN DIFFERENT FREQUENCIES

Frequency (kHz)	7.8125	15.625	31.25	62.5	125	250
Resistance (Ω/km)	19.3	35.5	63.8	112	191	318

This is demonstrated by multi-resolution analysis of wavelet transform. Fig. 6 shows the original current traveling wave with the sample rate of 1 MHz, and its wavelet modulus maxima under the scales 2^2, 2^4, and 2^6. These reflect the components of the traveling waves in sub-bands 250 kHz to 125 kHz, 62.5 kHz to 31.25 kHz, and 15.625 kHz to 7.8125 kHz.

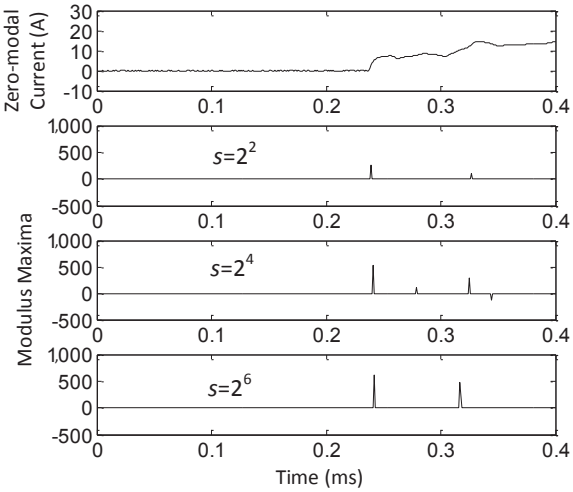

Fig. 6. Current fault traveling waves and its maximum modulus at different scales.

From Fig. 6, it is seen that for the lower frequency bands, the modulus maxima are higher. However, for larger scales, where $s > 2^6$, which corresponds to lower frequency bands, the exponent-decaying component and the power-frequency components dominate. The modulus maxima in these large scales should not be used. Considering these factors, using a sampling frequency of 1 MHz, the wavelet modulus maxima under the scale 2^6 (15.625 kHz to 7.8125 kHz) has been used for the protection.

D. Detailed Algorithm

The protection algorithm can be divided as follows:

Step 1: The zero-modal current and voltage traveling waves are acquired from current and voltage signals.

Step 2: Dyadic wavelet transforms is performed against zero-modal current and voltage traveling wave signals in order to extract the modulus maxima I_{M0} and U_{M0} for scale 2^6.

Step 3: The polarities of the modulus maxima of current and voltage traveling waves are compared.

Step 4: If the polarities of current and voltage traveling waves are opposite, then the magnitude of a power-frequency zero-sequence voltage U_0 is compared with a pre-set threshold U_{set}.

Step 5: If the magnitude of a power-frequency voltage U_0 is greater than U_{set}, then the sequence voltage based phase selection method is performed to distinguish single-phase-to-ground faults from two-phase-to ground faults.

Step 6: If a single-phase-to-ground fault is determined, a trip signal or alarm signal is issued.

Additionally, in order to avoid the procedure of the power frequency zero-sequence voltage based criterion from being frequently started up by noise, the protection is blocked when modulus maxima of the initial voltage or current traveling waves are less than a pre-set threshold $U_{\mathrm{M_{set}}}$ and $I_{\mathrm{M_{set}}}$. The thresholds values are determined by electromagnetic environment associated with the protection.:

In summary, operational logic of the protection is shown in Fig. 7.

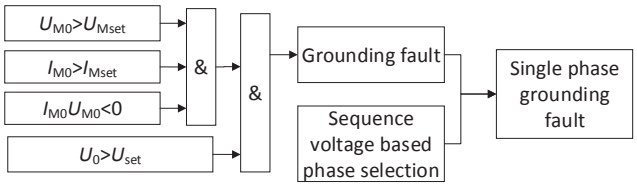

Fig. 7. Operation logic of the protection.

V. SIMULATION AND EVALUATION

The EMTP model of a power distribution system, used for simulation research, is described in section Section IV. B. The frequency-dependent parameters of a distribution line are taken into account. The modulus maxima are calculated for the faulty and healthy feeders L_2 and L_4, respectively, to demonstrate the validity of the above principle and algorithm for any feeder in the system.

A. Setting the Threshold Values of the Protection

As described above, there are two kinds of thresholds adopted in the protection algorithm in order to avoid the electromagnetic interference.

The noises caused by radiated or conducted interference are widely exiting in the substations. Under normal conditions, this kind of noise is much weaker than the traveling wave signal, but as it has a random characteristic, it might be misinterpreted as a traveling wave signal. In order to avoid it, the first kind of thresholds, $U_{\mathrm{M_{set}}}$ and $I_{\mathrm{M_{set}}}$, for modulus maxima are introduced. In this paper, the $U_{\mathrm{M_{set}}}$ and $I_{\mathrm{M_{set}}}$ are set as 10,000 and 100, respectively. Both thresholds can be adjusted allowing for the local electromagnetic conditions. The bigger the values of $U_{\mathrm{M_{set}}}$ and $I_{\mathrm{M_{set}}}$ are, the higher the reliability, but the lower the sensitivity of the protection.

In some situation, such as lightning strikes or switching transients, the induced noise signal can be so powerful that the value of its modulus maxima is higher than $U_{\mathrm{M_{set}}}$ and $I_{\mathrm{M_{set}}}$. To prevent the mal-operation of the protection under such conditions, the second threshold, U_{set}, associated with the value of a busbars voltage, is introduced. Normally, the

rated value of a secondary phase voltage is 57.7 V. From the field experience, the threshold $U_{\rm set}$ is set to 10 V. This value of the threshold also allows for handling voltage unbalances.

B. Behavior Under Different System Network Structure

A variety of faults was examined to demonstrate that the protection can be successfully used in any non-effectively grounded distribution system.

Table II shows the simulation results of phase A to ground faults modeled in test distribution systems. It can be concluded that the system network structure does not affect the operation of the protection, as the values of modulus maxima corresponding to current and voltage initial traveling waves change only a little. The column in Table II, titled Operation Result, presents results achieved for the faulty feeder.

TABLE II
BEHAVIOR UNDER DIFFERENT SYSTEM NETWORK STRUCTURES

Grounding Method	Faulty Feeder	$U_{\rm M0}$	$I_{\rm M0}$ Faulty Feeder	$I_{\rm M0}$ Healthy Feeder	Operation Result
Ungrounded	Main	-158,980	798	-182	Operating
Ungrounded	Branch	-97,775	640	-162	Operating
Resonant	Main	-156,750	787	-180	Operating
Resonant	Branch	-95,184	624	-158	Operating

The protection is also effective in meshed networks, as the structure of electric networks will not affect the criteria. As nearly all of the meshed electrical networks are usually operated as open-loop ones, only radial system is discussed in this paper.

It is necessary to point out that the protection criteria are also satisfied in case of an effectively grounded distribution system. However, as single-phase-to-ground faults can result in very high fault currents, the extraction of the current traveling waves might be difficult because of high levels of noise in a current signal. For this reason, the traditional zero-sequence over current protection, instead of the proposed one, is recommended in this case.

C. Behavior Under Different Fault Distances

Two extreme kinds of fault distances are considered. The first one is a fault close to the busbar and the second at the remote end of a feeder.

For the close-up fault, the immediate reflection of traveling waves between the busbar and the fault point could cause confusion when a relatively low sampling rate is applied. All performed simulations reported the correct operation of the proposed protection under such conditions. This indicates that the follow-up traveling waves have the same polarity as the initial traveling wave, which additionally contributes to the yield of even larger values of measured modulus maxima than those for other fault distances.

For the fault at the remote end of a feeder, the zero-modal traveling wave would be greatly attenuated at the relaying point. The higher frequency bands of a traveling wave then are also considerably attenuated for feeders longer than 20 km. The relatively lower frequency bands, however, are not affected so much and they are sufficient for analysis. In fact, most of the examined distribution lines were shorter than 20 km.

Table III shows the simulation results for different values of fault distances. The protection operates correctly in all cases.

TABLE III
BEHAVIOR UNDER DIFFERENT FAULT DISTANCES

Fault Distance (km)	$U_{\rm M0}$	$I_{\rm M0}$ Faulty Feeder	$I_{\rm M0}$ Healthy Feeder	Operation Result
0.5	-365,670	2,532	-570	Operating
5	-158,980	798	-182	Operating
20	-77,026	532	-136	Operating

D. Behavior Under Different Fault Inception Angles

Different fault inception angles, specifically those close to voltage zero-crossing, have been examined. Equation (10) clearly shows that there is a close relationship between the fault inception angle and amplitude of a traveling wave. Theoretically, traveling waves will be generated by any fault with non-zero inception angle. The results presented in Table IV show that when fault inception angles equal 10° or -10°, then all polarity criteria of the protection are well satisfied. But in case of the angle 10°, the measured modulus maxima $I_{\rm M0}$ for the faulty feeder is smaller than $I_{\rm M_{set}}$, and the protection does not operate. The local electromagnetic conditions around the protection should be considered better in order to specify more reliable values of pre-set thresholds for the protection blocking purposes.

TABLE IV
BEHAVIOR UNDER DIFFERENT FAULT VOLTAGE INCEPTION ANGLES

Inception Angle (°)	$U_{\rm M0}$	$I_{\rm M0}$ Faulty Feeder	$I_{\rm M0}$ Healthy Feeder	Operation Result
-10	35,178	-184	40	Operating
10	-23,619	94	-23	Not-operating
90	-158,980	798	-182	Operating

E. Behavior Under Different Fault Path Resistances

Phase A to ground faults with various fault path resistances have been examined in simulation research. The results are collected in Table V. It was found that the magnitudes of fault generated current and voltage traveling waves decreased when the fault path resistance increased. All the traveling waves are, however, still significant enough to make the protection operate as required.

F. The Limitations of the Protection

Many simulations carried out to test the proposed protection with overall consideration of a fault distance, fault inception angle, and fault path resistance changing over a wide range of values, 0.5 km to 20 km, 0° to 90° and 0.1 Ω to 400 Ω, respectively, as shown in Table VI, have offered insights into protection reliability.

TABLE V
BEHAVIOR UNDER DIFFERENT FAULT VOLTAGE INCEPTION ANGLES

Path Resistances (Ω)	U_{M0}	I_{M0} Faulty Feeder	I_{M0} Healthy Feeder	Operation Result
0.1	-158,980	798	-182	Operating
100	-103,570	619	-118	Not-operating
200	-78,007	508	-91	Operating
400	-56,432	373	-66	Operating

TABLE VI
BEHAVIOR UNDER DIFFERENT FAULT PARAMETERS

Inception angle ($\circ$)	Path Resistances(Ω)	Fault Distance (km)	U_{M0}	I_{M0} Healthy Feeder	Operation Result
10	0.1	0.5	-42,808	294	Operating
10	0.1	20	-8,802	60	Not-operating
10	400	0.5	-7,697	53	Not-operating
10	400	20	-4,866	32	Not-operating
30	0.1	0.5	-164,590	1138	Operating
30	0.1	20	-34,485	238	Operating
30	400	0.5	-29,694	208	Operating
30	400	20	-18,999	127	Operating
90	0.1	0.5	-365,670	2532	Operating
90	0.1	20	-77,026	532	Operating
90	400	0.5	-66,042	464	Operating
90	400	20	-42,387	284	Operating

The simulations show that the most important factor affecting the performance of the protection is a fault inception angle. The protection operates effectively for all values of fault resistance and fault distance when fault inception angle is bigger than 30°. When the fault inception angle's value is in the range from 10° to 30°, the reliability of the protection is lowered as it might refuse to act especially if bigger values of both, a fault resistance and fault distance occur simultaneously. Fortunately, most faults happen when the phase voltage approaches its maximum value. The protection can be said to be effective and reliable.

Additionally, it is important to stress that the correct operation of the proposed protection is conditioned by measurements of modulus maxima (associated with fault generated traveling waves). As the values of modulus maxima can be affected by many factors (like the fault distance, fault inception angle, and fault path resistances), there might occur some extreme conditions resulting in protection misoperation. Especially as declared in Section V. A, when the modulus maxima generated by weak traveling waves and powerful noise signals cannot be discriminated.

VI. CONCLUSION

A new traveling wave based single-phase-to-ground fault protection method applied in distribution feeders has been proposed in this paper. The protection uses the polarity comparison of zero-modal initial current and voltage traveling waves to identify a fault. The busbar voltage is additionally applied to enhance the protection's dependability and to discriminate between single-phase-to-ground and two-phase-to-ground faults.

Compared with existing methods, the proposed protection only acquires information of the protected feeder. It, however, does provide the required dependability and sensitivity of operation where the protection scheme can be embedded into one protective relay, and no extra hardware is required to be fitted into the power system.

The protection can work correctly under most single phase-to-ground faults in power distribution networks with different types of grounding, though it is not recommended to be used in the effective grounded power distribution system.

APPENDIX

A. Demonstration Using Karenbauer Matrix to Decouple Three Unbalanced Lines

The line parameters of power distribution lines in Fig. 2 can be calculated by EMTP when the three phase lines are unbalanced, yielding

$$\omega C = \begin{bmatrix} 0.2463 & -0.0393 & -0.0441 \\ -0.0393 & 0.2412 & -0.0529 \\ -0.0441 & -0.0529 & 0.2515 \end{bmatrix} \cdot 10^{-5}(\mathrm{S/km})$$

$$\omega L = \begin{bmatrix} 0.7557 & 0.3507 & 0.3636 \\ 0.3507 & 0.7560 & 0.3724 \\ 0.3636 & 0.3724 & 0.7557 \end{bmatrix} (\Omega/km) \tag{A1}$$

When Karenbauer matrix is used to decouple the three phase lines, we get

$$\omega^2 \boldsymbol{S}^{-1} LC \boldsymbol{S} = \begin{bmatrix} 0.2302 & 0.0102 & -0.0022 \\ 0.0014 & 0.1146 & 0 \\ 0 & -0.0002 & 0.115 \end{bmatrix} \cdot 10^{-5}$$

$$\omega^2 \boldsymbol{S} LC \boldsymbol{S}^{-1} = \begin{bmatrix} 0.2302 & 0.0014 & 0 \\ 0.0102 & 0.1146 & -0.0002 \\ -0.0022 & 0 & 0.115 \end{bmatrix} \cdot 10^{-5} \tag{A2}$$

where $\boldsymbol{S}$ is the Karenbauer matrix.

From (A2), we can see that the off-diagonal elements are only about one percent of diagonal elements. This error is acceptable. Therefore, the phase-to-modal transformations can still be used to decouple non-transposed electric lines with acceptable accuracy.

B. Electric Network Data of Fig. 1

The system short circuit capacity is 106.2 MVA. The lengths of feeders from L_1 to L_8, which are connected to the busbar, are of 21.159, 26.371, 2.446, 17.959, 5.431, 7.959, 8.804, and 14.067 km, respectively. Two tapped loads are connected to feeder L_1 at the 5^{th} km. The feeder is made of an aluminum wire and its unit resistance is 0.2422 Ω/km. The maximum sag of a feeder is 2 m. The earth's resistivity is 100 Ω/km.

REFERENCES

[1] P. Ackerman, "Ground selector for ungrounded three-phase distribution systems," *Transactions of the American Institute of Electrical Engineers*, vol. 42, no. 4, pp. 518–526, 1923.

[2] L. F. Hunt and J. Vivian, "Sensitive ground protection for radial distribution feeders," *Transactions of the American Institute of Electrical Engineers*, vol. 59, no. 2, pp. 84–90, 1940.

[3] Gross and E. TB, "Sensitive ground protection for transmission lines and distribution feeders," *Transactions of the American Institute of Electrical Engineers*, vol. 60, no. 11, pp. 968–971, 1941.

[4] "Sensitive ground protection," *Transactions of the American Institute of Electrical Engineers*, vol. 69, no. 1, pp. 473–476, 1950.

[5] J. Roberts, H. J. Altuve, and D. Hou, "Review of ground fault protection methods for grounded, ungrounded, and compensated distribution systems," in *Western Protective Relaying Conference*, 2001, pp. 1–40.

[6] S. Zhang, W. Li, and Z. Mi, "Review of protective principal and technique in distribution system with neutral non-effective grounding," *Information on Electric Power*, 1994.

[7] L. Sr and D. H, "High resistance grounding and fault finding on three phase three wire (delta) power systems," in *Textile, Fiber, and Film Industry Technical Conference*, 1997, pp. 5–8.

[8] K. Zhu, P. Zhang, W. Wang, and W. Xu, "Controlled closing of PT delta winding for identifying faulted lines," *IEEE Transactions on Power Delivery*, vol. 26, no. 1, pp. 79–86, 2011.

[9] J. Bergeal, L. Berthet, O. Grob, P. Bertrand, and B. Lacroix, "Single-phase faults on compensated neutral medium voltage networks," in *12th International Conference on Electricity Distribution, 1993. CIRED.* IET, May 17–31 1993, pp. 2.9/1–2.9/5.

[10] O. Chaari, M. Meunier, and F. Brouaye, "Wavelets: a new tool for the resonant grounded power distribution systems relaying," *IEEE Transactions on Power Delivery,*, vol. 11, no. 3, pp. 1301–1308, 1996.

[11] ——, "Principle of magnitude & phase comparison for micro-computer based small current fault feeder selection," *Information on Electric Power*, vol. 5, no. 2, pp. 15–19, 1994.

[12] X. Dong and S. Shi, "Identifying single phase to ground fault feeder in neutral non-effectively grounded distribution system using wavelet transform," *IEEE Transactions on Power Delivery*, vol. 23, no. 4, pp. 1829–1837, 2008.

[13] H. Neugebauer, "Ein neuartiges prinzip zum erfassen von kurzzeitigen erdschlssen mittels eines wanderwellenrichtungsanzeigers," *Siemens-Zeitschrift*, vol. 23, no. 4, pp. 272–302, 1936.

[14] M. Chamia and S. Liberman, "Ultra high speed relay for ehv/uhv transmission lines-development, design and application," *IEEE Transactions on Power Apparatus and Systems*, vol. 97, no. 6, pp. 2104–2116, 1978.

[15] X. Dong, W. Kong, and T. Cui, "Fault classification and faulted-phase selection based on the initial current traveling wave," *IEEE Transactions on Power Delivery*, vol. 24, no. 2, pp. 552–559, 2009.

[16] X. Dong, Y. Ge, and J. He, "Surge impedance relay," *IEEE Transactions on Power Delivery*, vol. 20, no. 2, pp. 1247–1256, 2005.

[17] X. Dong, S. Wang, and S. Shi, "Polarized current travelling-wave based directional relay," *IEEE Transactions on Power Delivery*, vol. 35, no. 21, pp. 78–83, 2011.

[18] S. X. Shi, X. Z. Dong, and S. X. Zhou, "Analysis of single-phase-to-ground fault generated initial traveling waves," in *Transmission and Distribution Conference and Exhibition: Asia and Pacific, 2005 IEEE/PES*. IEEE, 2005, pp. 1–4.

[19] S. X. Shi and X. Z. Dong, "Implementation and test of fault line selector using zero module current travelling waves," in *Universities Power Engineering Conference, 2007. UPEC 2007. 42nd International*. IEEE, 2007, pp. 248–251.

[20] X. Liu, K. Guo, G. Ye, H. Huang, F. Yang, and P. Chen, "Experimental study on the impulse-voltage transmission characteristics of inductive voltage transformers," *High Voltage Engineering*, vol. 37, no. 10, pp. 2385–2390, 2011.

[21] C. Zhou, Z. He, and G. Luo, "Transient simulation of electromagnetic potential transformer and analysis on its traveling wave transfer characteristics," *Power System Technology*, vol. 31, no. 2, pp. 84–89, 2007.

[22] X. Zeng, Z. Liu, M. Qu, and Y. Zhou, "Simulative analysis and experimental test of the transmission characteristics of transient traveling-wave in transformer," *Journal of Hunan Light Industry College*, vol. 1, no. 1, pp. 71–75, 2004.

[23] Z. Y. Xu, *New Type Distance Protection of Power Line*. Beijing, China: Water & Power Press, 2002.

[24] S. Mallat and W. L. Hwang, "Singularity detection and processing with wavelets," *IEEE Transactions on Information Theory*, vol. 38, no. 2, pp. 617–643, 1992.

Xinzhou Dong as born in Shanxi Province, China, in 1963. He received his B.E. degree in 1983, his M.E. degree in 1991, and a Ph.D. degree in 1996 from the Department of Electrical Engineering, Xi'an Jiaotong University, China. He did his Post-Doctoral research at the Electrical Engineering Station of Tianjin University from 1997 to 1998. Since February 1999, he has been employed by Tsinghua University, China. At present, he serves as a Professor of Tsinghua University, and the Director of Tsinghua-AREVA T&D Research Center. His research interests include protective relaying, fault location and application of wavelet transforms in power systems. He is author or co-author of more than 100 journal papers.

Jun Wang was born in Inner Mongolia, China, in 1986. He received his B.E. degree in 2008 and Ph.D. degree in 2013 from Tsinghua University, Beijing, China. Now he serves as an Engineer in Electric Power Planning & Engineering Institute. His main research interests are electric power planning and international energy cooperation.

Shenxing Shi received the B.S. and Ph.D. degrees in electrical engineering from Northeast Institute of Electrical Power, Jilin, China, and Tsinghua University, Beijing, China, in 1999 and 2006, respectively. His research interests are power system analysis, power system protection, as well as signal processing and wavelet-transform applications in power systems.

Bin Wang received the B.Sc. degree in electrical engineering from Shandong University of Technology, China, in 1999, and Ph.D. degree from Shandong University, China, in 2005. From July 2005 to Dec 2010, he has been working as a Post-Doctoral Fellow and Assistant Researcher in Tsinghua University, China. Now he serves as an Associate Professor in Tsinghua University, and his main research interests are transmission line protection and location, substation automation based on IEC61850, and power quality.

Dominik Bak received the M.Sc. and Ph.D. degrees from Wroclaw University of Technology, Poland, in 2001 and 2006, respectively. From July 2007 to Feb. 2010, he worked as a Research Professor in NTPC, Myongji University, South Korea. Currently, he is as an Associate Professor at Tsinghua University, China. His main research interests are adaptive measurement and protection algorithms.

Miles A. Redfern (M'79-'10) received his B.Sc. degree from Nottingham University in 1970 and Ph.D. degree from Cambridge University in 1976. In 1970, he joined British Railways Research, and in 1975, moved to GEC Measurements where he held various posts including Head of Research and Long Term Development and Overseas Sales Manager. In 1986, he joined Bath University and is a Senior Lecturer in the Department of Electronic and Electrical Engineering, University of Bath, Bath, UK. He is currently a member of the organizing committee for the IET International Conference on Developments in Power System Protection. His interests include electrical power systems, their protection and control, exploitation of renewable energy sources and industrial management.